



OxyEMG: an application for determination of the oxyspinel group end-members based on electron microprobe analyses

Gabriela R. Ferracutti¹, Lucía M. Asiain¹, Antonella S. Antonini^{2,3}, Juan E. Tanzola¹, and
M. Luján Ganuza^{2,3}

¹Instituto Geológico del Sur (INGEOSUR, CONICET-UNS), Departamento de Geología,
Universidad Nacional del Sur, San Juan 670, B8000ICN Bahía Blanca, Buenos Aires, Argentina

²Laboratorio de Investigación y Desarrollo en Visualización y Computación Gráfica (VyGLab),
Departamento de Ciencias e Ingeniería de la Computación, Universidad Nacional del Sur,
San Andrés 800, B8000ICN Bahía Blanca, Buenos Aires, Argentina

³Instituto de Ciencias e Ingeniería de la Computación (ICIC, CONICET-UNS),
Universidad Nacional del Sur, San Andrés 800, B8000ICN Bahía Blanca, Buenos Aires, Argentina

Correspondence: Gabriela R. Ferracutti (gferrac@uns.edu.ar)

Received: 8 May 2023 – Revised: 3 November 2023 – Accepted: 27 November 2023 – Published: 17 January 2024

Abstract. The Oxyspinel group End-Member Generator (OxyEMG) is an improved version of the EMG application. This new version allows for calculating, based on electron microprobe analysis (EMPA), the proportions of 31 end-member components in an oxyspinel composition. These components are MgAl₂O₄ (spinel), FeAl₂O₄ (hercynite), MnAl₂O₄ (galaxite), ZnAl₂O₄ (gahnite), NiAl₂O₄ (chihmingite), CuAl₂O₄ (thermaerogenite), MgFe₂O₄ (magnesioferrite), Fe₃O₄ (magnetite), MnFe₂O₄ (jacobsite), ZnFe₂O₄ (franklinite), NiFe₂O₄ (trevorite), CuFe₂O₄ (cuprospinel), FeMn₂O₄, MgMn₂O₄, Mn₃O₄ (hausmannite), ZnMn₂O₄ (hetaerolite), MgCr₂O₄ (magnesiocromite), FeCr₂O₄ (chromite), MnCr₂O₄ (manganocromite), ZnCr₂O₄ (zincocromite), NiCr₂O₄ (nichromite), CoCr₂O₄ (cochromite), MgV₂O₄ (magnesiocoulsonite), FeV₂O₄ (coulsonite), MnV₂O₄ (vuorelainenite), Co₃O₄ (guite), TiMg₂O₄ (qandilite), TiFe₂O₄ (ulvöspinel), SiMg₂O₄ (ringwoodite), SiFe₂O₄ (ahrensite) and GeFe₂O₄ (brunogeierite).

Compared with the older version, OxyEMG allows for (a) calculating 12 additional oxyspinel group end-member compositions (chihmingite, thermaerogenite, hausmannite, hetaerolite, FeMn₂O₄, MgMn₂O₄, cuprospinel, cochromite, guite, ringwoodite, ahrensite and brunogeierite), (b) discriminating the cation valency not only for Fe²⁺–Fe³⁺ but also for Mn²⁺–Mn³⁺ and Co²⁺–Co³⁺, and (c) changing the method to calculate the components of the magnetite and ulvöspinel prisms.

As in EMG, this new version is an application that does not require an installation process and was created with the purpose of performing calculations to obtain cation proportions (per formula unit, p.f.u.), end-members of the oxyspinel group, a ΣR^{3+} value, a ΣR^{2+} value, $\Sigma R^{3+} / \Sigma R^{2+}$ ratios, redistribution proportions for the corresponding end-members in the magnetite or ulvöspinel prisms, and a data validation section to check the results.

1 Introduction

According to Bosi et al. (2019) the oxyspinel group comprises 33 mineral species approved by the International Mineralogical Association (IMA), which are grouped into two subgroups as summarized in Table 1. The Oxyspinel group End-Member Generator (OxyEMG) application presented in this contribution not only allows for calculating 27 of these end-members but also includes chihmingite, which is a new mineral species (Hwang et al., 2022), and FeMn_2O_4 , MgMn_2O_4 and nichromite components (Table 1). The oxyspinel group is part of the spinel supergroup, all of which have the general formula AB_2X_4 .

OxyEMG calculates the cation proportions per formula unit (p.f.u); 31 end-members of the oxyspinel group; and, when it is possible, the redistribution proportions of the end-members, with data required to plot a given dataset in the magnetite or ulvöspinel prisms.

2 Procedure considerations

The calculations of the oxyspinel end-members were carried out according to the following statements.

1. The oxyspinel group is a complex solid solution due to the substitution of chemical elements in their structure. For this reason the mineral species can have many empirical formulas. For example, spinel composition belonging to jacobsite, ideally MnFe_2O_4 , can be described by many empirical formulas that are Mn- and Fe-dominant. This is correct because names are assigned according to the dominant-valency rule in the formula (Hatert and Burke, 2008). In this work we will not use hypothetical end-members, i.e., those not identified as dominant component in the spinel minerals so far.
2. For the methodology applied to determine cation values from chemical analyses, see the previous version of EMG (Ferracutti et al., 2015).
3. As well as in EMG, in OxyEMG the Fe^{3+} – Fe^{2+} ratio estimation is carried out according to the methodology of Droop (1987), and the spinel (s.l.) data published by this author were again used as a reference to make all the calculations described in this paper (Tables 2 and S1–S6 in the Supplement).

After the discrimination indicated for Fe, in those cases where the oxidation does not provide the number of cations necessary to complete the structure, Mn^{2+} began to be oxidized to Mn^{3+} . After that, the same procedure was made for Co^{2+} – Co^{3+} .

The way to calculate cations such as Fe^{3+} , Mn^{3+} and Co^{3+} allows the users to observe the participation and the solid solution among end-members of the systems

MgAl_2O_4 – MgMn_2O_4 – MnMn_2O_4 (Bosi et al., 2010) and FeMn_2O_4 – MnFe_2O_4 – NiFe_2O_4 (Nepal, 2020) that otherwise would not be possible. For this reason it was necessary to incorporate FeMn_2O_4 and MgMn_2O_4 end-member compositions.

4. The application allows the user to choose if they want OxyEMG to provide the stoichiometric calculation of Fe_2O_3 – FeO and/or Mn_2O_3 – MnO and/or Co_2O_3 – CoO . However, if the user previously determined them by another methodology, OxyEMG can also be used to calculate the 31 oxyspinel group end-members. However, the authors strongly recommend using the data obtained with EMPA for the calculations. Examples are included (Tables S3, S4 and S5) to verify the results obtained when oxide discrimination is introduced by the user compared to when discrimination is made by the application (samples 2A and 8B from Bosi et al., 2002; Mn80B, Mn100B and Mn60E from Bosi et al., 2010; MgMn01 and MgMn10 from Bosi et al., 2007).
5. Dellagiustaita, deltalumite, maghemite, titanomaghemite, filipstadite and tegengrenite have not been calculated because obtaining results for these end-members requires the application to perform a lot of formulas and conditioning, due to the possible existence of solid solutions with other end-members. Besides that, there are few microprobe data available regarding these rare end-members which make it difficult to verify if the calculations made by OxyEMG are correct.
6. The sum of the 31 oxyspinel group end-members is 8, considering the formula unit based on four oxygens and three cations (see explanation in Ferracutti et al., 2015).
7. In order to choose which prism should be used to plot the output data, we have introduced three conditions based on Bosi et al. (2019).
 - A. If $\Sigma\text{R}^{3+} > 1.0$, $\Sigma\text{R}^{2+} < 1.5$ and $\Sigma\text{R}^{3+} / \Sigma\text{R}^{2+}$ varies from 2/3 to 2.0, the data should be plotted in the magnetite prism.
 - B. If $\Sigma\text{R}^{3+} < 1.0$, $\Sigma\text{R}^{2+} > 1.5$ and $\Sigma\text{R}^{3+} / \Sigma\text{R}^{2+}$ varies from 0 to 2/3, the data should be plotted in the ulvöspinel prism.

Bosi et al. (2019) introduced these conditions in order to determine which oxyspinel subgroup (2-3 or 4-2) the analyzed crystals correspond to. However, as the application was tested with oxyspinel group end-members and the objective is to know which of the data can be introduced or plotted in binary diagrams of the magnetite or ulvöspinel prisms, the limit value used for $\Sigma\text{R}^{3+} / \Sigma\text{R}^{2+}$ was ≤ 2.0 , instead of the < 2.0 suggested by Bosi et al. (2019). This change is due to the fact that in the case of the oxyspinel group end-members

Table 1. A total of 34 mineral species from the oxyspinel group and FeMn_2O_4 , MgMn_2O_4 and nichromite (NiCr_2O_4), which correspond to chemical components (modified from Bosi et al., 2019). Those with * are calculated with OxyEMG.

Oxyspinel group				
Spinel subgroup (2-3)	A ²⁺	B ³⁺	X	End-member calculated with OxyEMG
Chromite	Fe	Cr ₂	O ₄	*
Chihmingite	Ni	Al ₂	O ₄	*
Cochromite	Co	Cr ₂	O ₄	*
Coulsonite	Fe	V ₂	O ₄	*
Cuprospinel	Cu	Fe ₂	O ₄	*
Dellagiustaita	V	Al ₂	O ₄	*
Deltalumite	(Al _{0.67} □ _{0.33})	Al ₂	O ₄	*
FeMn ₂ O ₄	Fe	Mn ₂	O ₄	*
Franklinite	Zn	Fe ₂	O ₄	*
Gahnite	Zn	Al ₂	O ₄	*
Galaxite	Mn	Al ₂	O ₄	*
Guite	Co	Co ₂	O ₄	*
Hausmannite	Mn	Mn ₂	O ₄	*
Hercynite	Fe	Al ₂	O ₄	*
Hetaerolite	Zn	Mn ₂	O ₄	*
Jacobsite	Mn	Fe ₂	O ₄	*
Maghemite	(Fe _{0.67} ³⁺ □ _{0.33})	Fe ₂	O ₄	*
Magnesiochromite	Mg	Cr ₂	O ₄	*
Magnesiocoulsonite	Mg	V ₂	O ₄	*
Magnesioferrite	Mg	Fe ₂	O ₄	*
Magnetite	Fe	Fe ₂	O ₄	*
Manganochromite	Mn	Cr ₂	O ₄	*
MgMn ₂ O ₄	Mg	Mn ₂	O ₄	*
Nichromite	Ni	Cr ₂	O ₄	*
Spinel	Mg	Al ₂	O ₄	*
Thermaerogenite	Cu	Al ₂	O ₄	*
Titanomaghemite	(Ti _{0.5} ⁴⁺ □ _{0.5})	Fe ₂	O ₄	*
Trevorite	Ni	Fe ₂	O ₄	*
Vuorelainenite	Mn	V ₂	O ₄	*
Zincochromite	Zn	Cr ₂	O ₄	*
Ulvöspinel subgroup (4-2)	A ⁴⁺	B ²⁺	X	
Ahrensite	Si	Fe ₂	O ₄	*
Brunogeierite	Ge	Fe ₂	O ₄	*
Filipstadite	(Fe _{0.5} ³⁺ Sb _{0.5} ⁵⁺)	Mn ₂	O ₄	*
Qandilite	Ti	Mg ₂	O ₄	*
Ringwoodite	Si	Mg ₂	O ₄	*
Tegengrenite	(Mn _{0.5} ³⁺ Sb _{0.5} ⁵⁺)	Mg ₂	O ₄	*
Ulvöspinel	Ti	Fe ₂	O ₄	*

from the magnetite prism, the $\Sigma\text{R}^{3+} / \Sigma\text{R}^{2+}$ ratio is 2.0 ($\Sigma\text{R}^{3+} = 2.0$ and $\Sigma\text{R}^{2+} = 1.0$), and the condition < 2.0 would exclude that value (Table S4). According to that, OxyEMG will only perform the calculations of the end-members proportions if the three conditions are accomplished in each case.

For the output data in the magnetite or ulvöspinel prisms, the ΣR^{3+} and ΣR^{2+} in the OxyEMG application refer only to $\text{Al}^{3+} + \text{Fe}^{3+} + \text{Cr}^{3+}$ and to

$\text{Mg}^{2+} + \text{Fe}^{2+}$, respectively. If Mn^{2+} , Zn^{2+} , Cu^{2+} , Co^{2+} or other cations want to be considered in ΣR^{2+} or if V^{3+} , Si^{4+} or Ge^{4+} want to be included in ΣR^{3+} , the resulting composition could be represented in the magnetite or ulvöspinel prisms, but that would not be correct. Considering, e.g., jacobsite (Anthony et al., 2001–2005), $\Sigma\text{R}^{3+} = \text{Al}^{3+} + \text{Fe}^{3+} + \text{Cr}^{3+} = 2$, $\Sigma\text{R}^{2+} = \text{Mg}^{2+} + \text{Fe}^{2+} + \text{Mn}^{2+} = 1$ and $\Sigma\text{R}^{3+} / \Sigma\text{R}^{2+} = 2$, and based on the conditions

indicated before, the sample should be included in the magnetite prism. For this reason and in order to avoid incorrect assignments, we use $\text{Al}^{3+} + \text{Fe}^{3+} + \text{Cr}^{3+}$ for ΣR^{3+} and $\text{Mg}^{2+} + \text{Fe}^{2+}$ for ΣR^{2+} values. According to that, for the same example of $\Sigma\text{R}^{3+} = \text{Al}^{3+} + \text{Fe}^{3+} + \text{Cr}^{3+} = 2$, $\Sigma\text{R}^{2+} = \text{Mg}^{2+} + \text{Fe}^{2+} = 0.57$ and $\Sigma\text{R}^{3+} / \Sigma\text{R}^{2+} = 3.5$ two of the three conditions are accomplished. Therefore, there will be no values for none of the end-member in the prisms (Tables S3, S4 and S5).

8. If the dataset introduced by the user has end-member compositions plotting in the base of the prism (spinel, magnesiochromite, chromite and hercynite) or solid solutions among them, with the contents of Fe_2O_3 or TiO_2 wt % being equal to 0, the dataset will be plotted on the magnetite prism according to the conditions mentioned before (Tables S3, S4 and S5).
9. OxyEMG incorporates new 58 “data validation” options, allowing the user to verify if the calculations of their input data are well computed. The data validation is accomplished considering 87 ratios between the following end-members: $\text{FeAl}_2\text{O}_4/\text{MgAl}_2\text{O}_4$, $\text{FeFe}_2\text{O}_4/\text{MgFe}_2\text{O}_4$, $\text{FeCr}_2\text{O}_4/\text{MgCr}_2\text{O}_4$, $\text{FeV}_2\text{O}_4/\text{MgV}_2\text{O}_4$, $\text{Fe}_2\text{SiO}_4/\text{Mg}_2\text{SiO}_4$, $\text{TiFe}_2\text{O}_4/\text{TiMg}_2\text{O}_4$, $\text{FeMn}_2\text{O}_4/\text{MgMn}_2\text{O}_4$, $\text{MnAl}_2\text{O}_4/\text{FeAl}_2\text{O}_4$, $\text{MnFe}_2\text{O}_4/\text{FeFe}_2\text{O}_4$, $\text{MnCr}_2\text{O}_4/\text{FeCr}_2\text{O}_4$, $\text{MnV}_2\text{O}_4/\text{FeV}_2\text{O}_4$, $\text{MnMn}_2\text{O}_4/\text{FeMn}_2\text{O}_4$, $\text{MnAl}_2\text{O}_4/\text{MgAl}_2\text{O}_4$, $\text{MnFe}_2\text{O}_4/\text{MgFe}_2\text{O}_4$, $\text{MnCr}_2\text{O}_4/\text{MgCr}_2\text{O}_4$, $\text{MnV}_2\text{O}_4/\text{MgV}_2\text{O}_4$, $\text{MnMn}_2\text{O}_4/\text{MgMn}_2\text{O}_4$, $\text{MgCr}_2\text{O}_4/\text{MgAl}_2\text{O}_4$, $\text{FeCr}_2\text{O}_4/\text{FeAl}_2\text{O}_4$, $\text{MnCr}_2\text{O}_4/\text{MnAl}_2\text{O}_4$, $\text{ZnCr}_2\text{O}_4/\text{ZnAl}_2\text{O}_4$, $\text{NiCr}_2\text{O}_4/\text{NiAl}_2\text{O}_4$, $\text{MgFe}_2\text{O}_4/\text{MgAl}_2\text{O}_4$, $\text{FeFe}_2\text{O}_4/\text{FeAl}_2\text{O}_4$, $\text{MnFe}_2\text{O}_4/\text{MnAl}_2\text{O}_4$, $\text{ZnFe}_2\text{O}_4/\text{ZnAl}_2\text{O}_4$, $\text{NiFe}_2\text{O}_4/\text{NiAl}_2\text{O}_4$, $\text{CuFe}_2\text{O}_4/\text{CuAl}_2\text{O}_4$, $\text{MgFe}_2\text{O}_4/\text{MgCr}_2\text{O}_4$, $\text{FeFe}_2\text{O}_4/\text{FeCr}_2\text{O}_4$, $\text{MnFe}_2\text{O}_4/\text{MnCr}_2\text{O}_4$, $\text{ZnFe}_2\text{O}_4/\text{ZnCr}_2\text{O}_4$, $\text{NiFe}_2\text{O}_4/\text{NiCr}_2\text{O}_4$, $\text{Mg}_2\text{TiO}_4/\text{MgAl}_2\text{O}_4$, $\text{Fe}_2\text{TiO}_4/\text{FeAl}_2\text{O}_4$, $\text{Mg}_2\text{TiO}_4/\text{MgCr}_2\text{O}_4$, $\text{Fe}_2\text{TiO}_4/\text{FeCr}_2\text{O}_4$, $\text{MgV}_2\text{O}_4/\text{MgAl}_2\text{O}_4$, $\text{FeV}_2\text{O}_4/\text{FeAl}_2\text{O}_4$, $\text{MnV}_2\text{O}_4/\text{MnAl}_2\text{O}_4$, $\text{MgMn}_2\text{O}_4/\text{MgAl}_2\text{O}_4$, $\text{FeMn}_2\text{O}_4/\text{FeAl}_2\text{O}_4$, $\text{MnMn}_2\text{O}_4/\text{MnAl}_2\text{O}_4$, $\text{ZnMn}_2\text{O}_4/\text{ZnAl}_2\text{O}_4$, $\text{MgMn}_2\text{O}_4/\text{MgCr}_2\text{O}_4$, $\text{FeMn}_2\text{O}_4/\text{FeCr}_2\text{O}_4$, $\text{MnMn}_2\text{O}_4/\text{MnCr}_2\text{O}_4$, $\text{ZnMn}_2\text{O}_4/\text{ZnCr}_2\text{O}_4$, $\text{MgMn}_2\text{O}_4/\text{MgFe}_2\text{O}_4$, $\text{FeMn}_2\text{O}_4/\text{FeFe}_2\text{O}_4$, $\text{MnMn}_2\text{O}_4/\text{MnFe}_2\text{O}_4$, $\text{ZnMn}_2\text{O}_4/\text{ZnFe}_2\text{O}_4$, $\text{MgMn}_2\text{O}_3/\text{MgV}_2\text{O}_4$, $\text{FeMn}_2\text{O}_4/\text{FeV}_2\text{O}_4$, $\text{MnMn}_2\text{O}_4/\text{MnV}_2\text{O}_4$, $\text{MgFe}_2\text{O}_4/\text{MgV}_2\text{O}_4$, $\text{FeFe}_2\text{O}_4/\text{FeV}_2\text{O}_4$, $\text{MnFe}_2\text{O}_4/\text{MnV}_2\text{O}_4$, $\text{ZnAl}_2\text{O}_4/\text{FeAl}_2\text{O}_4$, $\text{ZnFe}_2\text{O}_4/\text{FeFe}_2\text{O}_4$, $\text{ZnCr}_2\text{O}_4/\text{FeCr}_2\text{O}_4$, $\text{ZnAl}_2\text{O}_4/\text{MgAl}_2\text{O}_4$, $\text{ZnFe}_2\text{O}_4/\text{MgFe}_2\text{O}_4$, $\text{ZnCr}_2\text{O}_4/\text{MgCr}_2\text{O}_4$, $\text{ZnAl}_2\text{O}_4/\text{MnAl}_2\text{O}_4$,



Figure 1. Screenshot of OxyEMG’s user interface.

$\text{ZnFe}_2\text{O}_4/\text{MnFe}_2\text{O}_4$, $\text{ZnCr}_2\text{O}_4/\text{MnCr}_2\text{O}_4$,
 $\text{CuAl}_2\text{O}_4/\text{FeAl}_2\text{O}_4$, $\text{CuFe}_2\text{O}_4/\text{FeFe}_2\text{O}_4$,
 $\text{CuAl}_2\text{O}_4/\text{MgAl}_2\text{O}_4$, $\text{CuFe}_2\text{O}_4/\text{MgFe}_2\text{O}_4$,
 $\text{CuAl}_2\text{O}_4/\text{MnAl}_2\text{O}_4$, $\text{CuFe}_2\text{O}_4/\text{MnFe}_2\text{O}_4$,
 $\text{CuAl}_2\text{O}_4/\text{ZnAl}_2\text{O}_4$, $\text{CuFe}_2\text{O}_4/\text{ZnFe}_2\text{O}_4$,
 $\text{NiAl}_2\text{O}_4/\text{FeAl}_2\text{O}_4$, $\text{NiFe}_2\text{O}_4/\text{FeFe}_2\text{O}_4$,
 $\text{NiCr}_2\text{O}_4/\text{FeCr}_2\text{O}_4$, $\text{NiAl}_2\text{O}_4/\text{MgAl}_2\text{O}_4$,
 $\text{NiFe}_2\text{O}_4/\text{MgFe}_2\text{O}_4$, $\text{NiCr}_2\text{O}_4/\text{MgCr}_2\text{O}_4$,
 $\text{NiAl}_2\text{O}_4/\text{MnAl}_2\text{O}_4$, $\text{NiFe}_2\text{O}_4/\text{MnFe}_2\text{O}_4$,
 $\text{NiCr}_2\text{O}_4/\text{MnCr}_2\text{O}_4$, $\text{NiAl}_2\text{O}_4/\text{ZnAl}_2\text{O}_4$,
 $\text{NiFe}_2\text{O}_4/\text{ZnFe}_2\text{O}_4$ and $\text{NiCr}_2\text{O}_4/\text{ZnCr}_2\text{O}_4$.

Underlined ratios are the new data validations included in OxyEMG compared with the previous version of EMG (Ferracutti et al., 2015). Examples are provided in Table S6.

In order to check the results provided by OxyEMG, the four examples indicated by Bosi et al. (2019) were represented, achieving the same results as those obtained by these authors (Table S4).

3 Application description

OxyEMG does not require an installation process. The user must download the application folder in their computer and execute the OxyEMG.exe file. Once the interface is loaded, OxyEMG is ready to be used. Figure 1 shows the application user interface, which supports the loading of .csv files by clicking a simple button.

The .csv source file must contain the information in columns, with one column containing the sample name and the others containing the wt % oxides (Table 2). It is not required that the oxides follow a fixed order or all to be present, but the “sample” name column must be present. OxyEMG considers the SiO_2 , TiO_2 , GeO_2 , Al_2O_3 , Cr_2O_3 , V_2O_3 , Fe_2O_3 , FeO , Mn_2O_3 , Co_2O_3 , MnO , MgO , CaO , ZnO , NiO , CuO and CoO oxides. If some of these oxides are missing in the input file, a warning message is displayed (Fig. 2) and a value of 0 will be assumed for the missing oxides.

Table 2. Oxide labels for .csv input files.

Sample	SiO ₂	TiO ₂	GeO ₂	Al ₂ O ₃	Cr ₂ O ₃	V ₂ O ₃	Fe ₂ O ₃	Mn ₂ O ₃	Co ₂ O ₃	FeO
Droop (1987) data	0.00	0.00	0.00	61.99	0.00	0.00	0.00	0.00	0.00	24.68
Coulsonite	0.00	0.00	0.00	0.00	0.00	67.60	0.00	0.00	0.00	32.40
Magnesiocromite	0.00	0.00	0.00	0.00	79.04	0.00	0.00	0.00	0.00	0.00
Chromite	0.00	0.00	0.00	0.00	67.90	0.00	0.00	0.00	0.00	32.10
Zincochromite	0.00	0.00	0.00	0.00	65.13	0.00	0.00	0.00	0.00	0.00
Ulvöspinel	0.00	35.73	0.00	0.00	0.00	0.00	0.00	0.00	0.00	64.27
Spinel	0.00	0.00	0.00	71.67	0.00	0.00	0.00	0.00	0.00	0.00
Magnesiocoulsonite	0.00	0.00	0.00	0.00	0.00	78.81	0.00	0.00	0.00	0.00
Hercynite	0.00	0.00	0.00	58.66	0.00	0.00	0.00	0.00	0.00	41.34
Gahnite	0.00	0.00	0.00	55.61	0.00	0.00	0.00	0.00	0.00	0.00
Trevorite	0.00	0.00	0.00	0.00	0.00	0.00	68.13	0.00	0.00	0.00
Magnetite	0.00	0.00	0.00	0.00	0.00	0.00	68.97	0.00	0.00	31.03
Magnesioferrite	0.00	0.00	0.00	0.00	0.00	0.00	79.85	0.00	0.00	0.00
Jacobsite	0.00	0.09	0.00	0.00	0.00	0.00	73.96	0.00	0.00	2.57
Franklinite	0.00	0.70	0.00	1.25	0.00	0.00	63.90	0.00	0.00	3.60
Manganochromite	0.00	0.00	0.00	0.00	62.30	1.70	0.00	0.00	0.00	9.40
Galaxite	0.96	0.00	0.00	45.71	0.00	0.00	0.00	0.00	0.00	16.36
Qandilite, T5, Bosi et al. (2014)	0.00	40.18	0.00	0.00	0.00	0.00	0.00	0.00	0.00	40.06
Cuprospinel	0.00	0.00	0.00	2.6	0.00	0.00	65.7	0.00	0.00	1.7
Ringwoodite	38.9	0.00	0.00	0.00	0.00	0.00	0.00	0.00	0.00	23.40
Ahrensite	34.9	0.00	0.00	0.00	0.00	0.00	0.00	0.00	0.00	43.8
Brunogeierite	0.00	0.00	42.13	0.00	0.00	0.00	0.00	0.00	0.00	57.87
Thermaerogenite	0.00	0.00	0.00	56.17	0.00	0.00	0.00	0.00	0.00	0.00
Cochromite, de Waal (1978)	0.11	1.26	0.00	9.11	50.38	0.00	0.00	0.00	0.00	11.18
Vuorelainenite	0.00	0.1	0.00	0.00	19.5	47.4	0.00	0.00	0.00	5.7
Nichromite, de Waal (1978)	0.20	1.13	0.00	7.46	45.56	0.00	0.00	0.00	0.00	17.32
No. 5, Oktyabrsky et al. (1992)	0.00	27.34	0.00	3.33	0.13	0.00	27.01	0.00	0.00	14.62
No. 3, Oktyabrsky et al. (1992)	0.00	21.07	0.00	4.85	0.00	0.00	39.28	0.00	0.00	1.44
FeTi30A, Bosi et al. (2009)	0.00	16.1	0.00	0.00	0.00	0.00	0.00	0.00	0.00	79.55
FeTi50Bd, Bosi et al. (2009)	0.00	20.14	0.00	0.61	0.00	0.00	0.00	0.00	0.00	73.83
RhumBA _n 2, Lenaz et al. (2011)	0.00	2.6	0.00	9	25.3	0.81	0.00	0.00	0.00	56.7
SC, Salamanca district Bjerg et al. (1993)	0.00	0.00	0.00	0.96	59.87	0.00	7.88	0.00	0.00	23.08
LTC, Las Tunas area Bjerg et al. (1993)	0.00	0.00	0.00	24.3	40.43	0.00	4.24	0.00	0.00	18.44
2A, Bosi et al. (2002) Mn discriminated	0.00	0.00	0.00	0.00	0.00	0.00	0.00	68.7	0.00	0.00

Table 2. Continued.

Sample	SiO ₂	TiO ₂	GeO ₂	Al ₂ O ₃	Cr ₂ O ₃	V ₂ O ₃	Fe ₂ O ₃	Mn ₂ O ₃	Co ₂ O ₃	FeO
8A, Bosi et al. (2002) Mn discriminated	0.00	0.00	0.00	0.12	0.00	0.00	0.00	68.5	0.00	0.00
2A, Bosi et al. (2002) Mn not discriminated	0.00	0.00	0.00	0.00	0.00	0.00	0.00	0.00	0.00	0.00
8A, Bosi et al. (2002) Mn not discriminated	0.00	0.00	0.00	0.12	0.00	0.00	0.00	0.00	0.00	0.00
Mn80B, Bosi et al. (2010) Mn discriminated	0.00	0.00	0.00	1.73	0.00	0.00	0.00	68.57	0.00	0.00
Mn100B, Bosi et al. (2010) Mn discriminated	0.00	0.00	0.00	0.00	0.00	0.00	0.00	69.70	0.00	0.00
Mn60E, Bosi et al. (2010) Mn discriminated	0.00	0.00	0.00	41.55	0.00	0.00	0.00	29.41	0.00	0.00
Mn100B, Bosi et al. (2010) Mn not discriminated	0.00	0.00	0.00	0.00	0.00	0.00	0.00	0.00	0.00	0.00
Mn60E, Bosi et al. (2010) Mn not discriminated	0.00	0.00	0.00	41.55	0.00	0.00	0.00	0.00	0.00	0.00
Sample b, Table 2 Antao et al. (2019)	0.00	0.00	0.00	0.00	0.00	0.00	16.55	52.37	0.00	0.00
S1, Table 3 Yavuz and Yavuz (2023)	0.01	0.22	0.00	1.02	24.99	39.98	0.00	0.00	0.00	27.21
Guite, S3, Table 3 Yavuz and Yavuz (2023)	0.54	0.00	0.00	0.00	0.00	0.00	0.00	0.00	0.00	0.00
N205, high Fe Gutzmer et al. (1995)	0.00	0.00	0.00	0.00	0.00	0.00	11.3	57.1	0.00	0.00
LVB404, low Fe Gutzmer et al. (1995)	0.00	0.00	0.00	0.00	0.00	0.00	1.2	65.2	0.00	0.00
MgMn01, Bosi et al. (2007) Mn not discriminated	0.00	0.00	0.00	71.10	0.00	0.00	0.00	0.00	0.00	0.00
MgMn10, Bosi et al. (2007) Mn not discriminated	0.00	0.00	0.00	60.00	0.00	0.00	0.00	0.00	0.00	0.00
MgMn01, Bosi et al. (2007) Mn discriminated	0.00	0.00	0.00	71.10	0.00	0.00	0.00	0.43	0.00	0.00
MgMn10, Bosi et al. (2007) Mn discriminated	0.00	0.00	0.00	60.00	0.00	0.00	0.00	11.06	0.00	0.00
Coulsonite I Kompanchenko (2020)	0.00	0.29	0.00	0.99	32.87	32.91	0.00	0.00	0.00	25.69
Coulsonite III Kompanchenko (2020)	0.05	0.54	0.00	2.46	28.04	28.51	0.00	0.00	0.00	35.82

Table 2. Continued.

Sample	MnO	MgO	CaO	ZnO	NiO	CuO	CoO
Droop (1987) data	0.11	13.70	0.00	0.00	0.00	0.00	0.00
Coulsonite	0.00	0.00	0.00	0.00	0.00	0.00	0.00
Magnesiochromite	0.00	20.96	0.00	0.00	0.00	0.00	0.00
Chromite	0.00	0.00	0.00	0.00	0.00	0.00	0.00
Zincochromite	0.00	0.00	0.00	34.87	0.00	0.00	0.00
Ulvöspinel	0.00	0.00	0.00	0.00	0.00	0.00	0.00
Spinel	0.00	28.33	0.00	0.00	0.00	0.00	0.00
Magnesiocoulsonite	0.00	21.19	0.00	0.00	0.00	0.00	0.00
Hercynite	0.00	0.00	0.00	0.00	0.00	0.00	0.00
Gahnite	0.00	0.00	0.00	44.39	0.00	0.00	0.00
Trevorite	0.00	0.00	0.00	0.00	31.87	0.00	0.00
Magnetite	0.00	0.00	0.00	0.00	0.00	0.00	0.00
Magnesioferrite	0.00	20.15	0.00	0.00	0.00	0.00	0.00
Jacobsite	13.94	9.26	0.00	0.00	0.00	0.00	0.00
Franklinite	0.60	0.00	0.00	30.25	0.00	0.00	0.00
Manganochromite	24.00	0.00	0.00	1.70	0.00	0.00	0.00
Galaxite	34.03	1.50	0.00	0.00	0.00	0.00	0.00
Qandilite, T5, Bosi et al. (2014)	0.00	19.49	0.00	0.00	0.00	0.00	0.00
Cuprospinel	0.20	1.80	0.00	0.70	0.00	27.8	0.60
Ringwoodite	0.00	37	0.00	0.00	0.00	0.00	0.00
Ahrensite	0.75	21.1	0.00	0.00	0.00	0.00	0.00
Brunogeierite	0.00	0.00	0.00	0.00	0.00	0.00	0.00
Thermaerogenite	0.00	0.00	0.00	0.00	0.00	43.83	0.00
Cochromite, de Waal (1978)	0.84	0.95	0.00	0.59	7.67	0.00	17.45
Vuorelainenite	26.4	0.1	0.00	0.8	0.00	0.00	0.00
Nichromite, de Waal (1978)	0.21	0.4	0.00	0.00	15.86	0.00	12.49
No. 5, Oktyabrsky et al. (1992)	1.89	26.47	0.00	0.00	0.00	0.00	0.00
No. 3, Oktyabrsky et al. (1992)	2.69	30.75	0.00	0.00	0.00	0.00	0.00
FeTi30A, Bosi et al. (2009)	0.00	0.00	0.00	0.00	0.00	0.00	0.00
FeTi50Bd, Bosi et al. (2009)	0.00	0.00	0.00	0.00	0.00	0.00	0.00
RhumBAn2, Lenaz et al. (2011)	0.38	2.64	0.00	0.09	0.34	0.00	0.00
SC, Salamanca district Bjerg et al. (1993)	0.00	2.71	0.00	4.99	0.00	0.00	0.00
LTC, Las Tunas area Bjerg et al. (1993)	0.00	9.73	0.00	0.87	0.00	0.00	0.00
2A, Bosi et al. (2002) Mn discriminated	27.9	0.4	0.00	2.5	0.00	0.00	0.00

Table 2. Continued.

Sample	MnO	MgO	CaO	ZnO	NiO	CuO	CoO
8A, Bosi et al. (2002) Mn discriminated	30.2	0.03	0.00	0.73	0.00	0.00	0.00
2A, Bosi et al. (2002) Mn not discriminated	89.6	0.4	0.00	2.5	0.00	0.00	0.00
8A, Bosi et al. (2002) Mn not discriminated	91.7	0.03	0.00	0.73	0.00	0.00	0.00
Mn80B, Bosi et al. (2010) Mn discriminated	23.73	4.70	0.00	0.00	0.00	0.00	0.00
Mn100B, Bosi et al. (2010) Mn discriminated	25.68	3.20	0.00	0.00	0.00	0.00	0.00
Mn60E, Bosi et al. (2010) Mn discriminated	11.69	17.28	0.00	0.00	0.00	0.00	0.00
Mn100B, Bosi et al. (2010) Mn not discriminated	88.32	3.20	0.00	0.00	0.00	0.00	0.00
Mn60E, Bosi et al. (2010) Mn not discriminated	38.12	17.28	0.00	0.00	0.00	0.00	0.00
Sample b, Table 2 Antao et al. (2019)	30.66	0.15	0.00	0.00	0.00	0.00	0.00
S1, Table 3 Yavuz and Yavuz (2023)	2.31	0.00	0.00	3.79	0.00	0.00	0.00
Guite, S3, Table 3 Yavuz and Yavuz (2023)	0.87	0.00	0.00	0.00	0.00	0.73	90.95
N205, high Fe Gutzmer et al. (1995)	31.80	0.00	0.00	0.00	0.00	0.00	0.00
LVB404, low Fe Gutzmer et al. (1995)	33.10	0.36	0.00	0.00	0.00	0.00	0.00
MgMn01, Bosi et al. (2007) Mn not discriminated	0.65	28.10	0.00	0.00	0.00	0.00	0.00
MgMn10, Bosi et al. (2007) Mn not discriminated	15.00	23.50	0.00	0.00	0.00	0.00	0.00
MgMn01, Bosi et al. (2007) Mn discriminated	0.26	28.10	0.00	0.00	0.00	0.00	0.00
MgMn10, Bosi et al. (2007) Mn discriminated	5.24	23.50	0.00	0.00	0.00	0.00	0.00
Coulsonite I Kompanchenko (2020)	2.34	0.00	0.00	4.48	0.00	0.00	0.00
Coulsonite III Kompanchenko (2020)	0.09	0.00	0.00	4.12	0.00	0.00	0.00

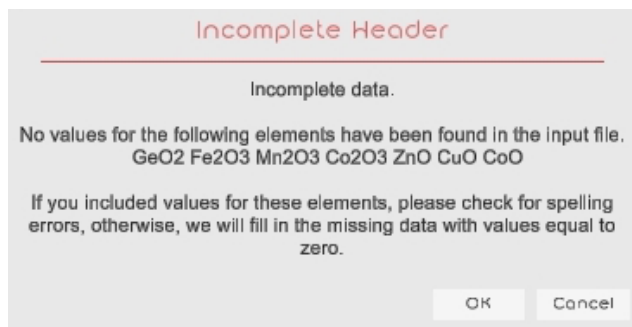


Figure 2. Example of warning message indicating that GeO_2 , V_2O_3 , Fe_2O_3 , Mn_2O_3 , Co_2O_3 , ZnO , CuO and CoO data are not present.

For Fe_2O_3 , Mn_2O_3 and Co_2O_3 to be calculated based on the FeO , MnO and CoO content, respectively, the user must type 0 in the column of Fe_2O_3 , Mn_2O_3 and Co_2O_3 . On the other hand, if the user has previously determined the values of Fe_2O_3 – FeO , Mn_2O_3 – MnO and Co_2O_3 – CoO , oxides values must be included in the corresponding columns, but for the calculations we strongly recommend using the data obtained with EMPA.

After loading the source file, if the format of the file is correct, a “selection” window is shown (Fig. 3), allowing the user to select the results that they require to include in the output files. OxyEMG supports calculations for the stoichiometric discrimination between Fe_2O_3 – FeO , Mn_2O_3 – MnO and Co_2O_3 – CoO (wt %) (Table S1); the cation proportions (p.f.u.) (Table S2); the end-members of the oxyspinel group (Table S3); the ΣR^{3+} value; the ΣR^{2+} value; and $\Sigma\text{R}^{3+} / \Sigma\text{R}^{2+}$ ratios (Table S4). It also provides recalculation of the end-members for the magnetite or ulvöspinel prisms (Table S5) and the option to perform a data validation (Table S6). The data validation conducts a test to verify if the calculated data results are correct.

Once the selection is made, OxyEMG performs the corresponding calculations, generates the output files and saves them in the same directory as the source file.

4 Important considerations when using OxyEMG

In general, the considerations indicated for the use of the previous version (EMG; Ferracutti et al., 2015) are valid in OxyEMG as well; however there are some new considerations that must be taken into account.

1. The “sample” name must be listed in one column of the .csv file, as it was also required in the previous version, but be careful to type “sample” (singular) and not “samples” (plural).
2. In OxyEMG, the only oxides values (wt %) that will be considered for the calculations are SiO_2 , TiO_2 , GeO_2 ,

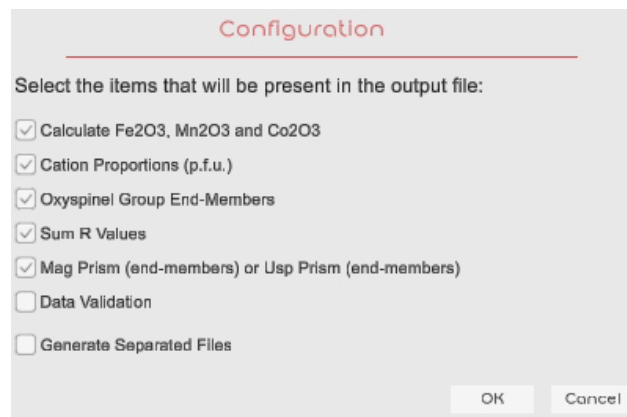


Figure 3. The selection windows allows the user to select the calculations that they require to be included in the output files.

Al_2O_3 , Cr_2O_3 , V_2O_3 , Fe_2O_3 , FeO , MnO , MgO , CaO , ZnO , NiO , CuO and CoO . In this new version GeO_2 , Mn_2O_3 , Co_2O_3 , CuO and CoO were added because they are required to calculate some oxyspinel group end-members such as thermaerogenite, cuprospinel, cochromite, brunogeierite, guite, hausmannite, hetaerolite, FeMn_2O_4 and MgMn_2O_4 . In OxyEMG Na_2O and K_2O are excluded because they are not part of any of the oxyspinel group end-members.

3. According to the previous consideration and the conditions indicated in item 4 of “Procedure considerations”, when a user introduces a composition of oxyspinel group end-member with values for SiO_2 , GeO_2 , MnO , V_2O_3 , Mn_2O_3 , Co_2O_3 , NiO , ZnO , CuO and/or CoO , the program will not discriminate between the two prisms because at least one of the indicated conditions is not accomplished. The reason for this is that the data used in the calculations comprise oxides of an oxyspinel end-member different from the ones included in the prisms; examples are the Salamanca (SC) and Las Tunas area (LTC) samples (Bjerg et al., 1993) included in Tables S3, S4 and S5. However, if the user has oxyspinel group end-members with negligible amounts of Si, Ge, V, Mn, Zn, Ni, Co, and/or Cu and they would like to determine their proportions referring to the magnetite or ulvöspinel prisms, with the proportion established for the 31 final members, they will have to make the necessary recalculation.
4. To test the OxyEMG program, oxyspinel group end-member’s data were taken from de Waal (1978), Droop (1987), Oktyabrsky et al. (1992), Bjerg et al. (1993), Gutzmer et al. (1995), the Handbook of Mineralogy .pdf files (Anthony et al., 2001–2005), Bosi et al. (2002, 2009, 2010, 2014), Lenaz et al. (2011), Antao et al. (2019), Kompanchenko (2020), and Yavuz and Yavuz (2023) (Tables S1–S6).

5 Discussion

As mentioned before, OxyEMG calculates cation end-member proportions from crystal analyzed by EMPA. This application neither assigns a mineral species for the crystal nor gives an ideal end-member formula. However, OxyEMG allows the user to observe which end-members are involved and in what proportion they are found. In this way, it is up to the user to assign a mineral species to their crystals, depending on the criterion they opt to utilize. They can choose the rule of the dominant valency or the rule of 50%. This approach helps to prevent any uncertainties that may arise when dealing with a significant number of hypothetical end-members, which could potentially generate a multitude of variants. Consequently, as reported in Table 1 of Dolivo-Dobrovolsky (2010), defining the mineral species based on the dominant end-member becomes a challenge due to the resulting ambiguity.

The authors consider that it is more important to provide the user with the composition and proportion of all the end-members that constitute the crystal than the name of the mineral species, which ultimately can still be assigned by the user. For example, based on the dominant-valency rule, coulsonite I and III (Kompanchenko, 2020), included in Tables S3, S4 and S5, effectively correspond to coulsonite, given that the dominant A cation is Fe^{2+} (0.8 and 0.9, respectively) and the dominant B cation is V (0.98 and 0.84, respectively). However, considering the proportions of the end-members, it is gathered that although coulsonite is the most abundant (3.357 and 3.163, respectively), there are other end-members in the structure, such as chromite (3.306 and 3.068, respectively), whose proportions are very close to the dominant one.

A program called WinSpingc (Yavuz and Yavuz, 2023) has recently been published which calculates the cations (a.p.f.u, atoms per formula unit) for all end-members of the spinel supergroup (oxyspinel, thiospinel and selenospinel groups) and defines the mineral species based on the dominant A cations and dominant B cations. However, the proportions of the all end-members present in the analyzed crystals are not determined.

Other differences between WinSpingc and OxyEMG include the Fe^{3+} , Mn^{3+} and Co^{3+} determination. In WinSpingc these cations are calculated entirely by the Droop (1987) methodology, considering each of them independently of the presence of another, and, therefore, it is not possible to determine the coexistence of, for example, Fe^{3+} – Mn^{3+} or Mn^{3+} – Co^{3+} . This was tested considering sample S3 from Table 3 (Guite, Yavuz and Yavuz, 2023), which according to WinSpingc, only has Co^{3+} as a dominant B cation. However, according to OxyEMG, this sample consists mainly of Co^{3+} with a very low participation of Mn^{3+} (Tables S3, S4 and S5). This agrees with Lei et al. (2022), who studied guite crystals (guite sample from Yavuz and Yavuz, 2023, is an av-

erage of samples from Lei et al., 2022) and also indicated the presence of Mn^{3+} in B.

Finally, WinSpingc calculates, according to Bosi et al. (2019), ΣR^{2+} (all divalent cations: $\text{Mg}^{2+} + \text{Fe}^{2+} + \text{Mn}^{2+} + \text{Cu}^{2+} + \text{Zn}^{2+} + \text{Co}^{2+} + \text{Ni}^{2+} + \text{V}^{2+}$) and ΣR^{3+} (all trivalent cations: $\text{Cr}^{3+} + \text{Fe}^{3+} + \text{Al}^{3+} + \text{Mn}^{3+} + \text{Co}^{3+}$) to determine to which oxyspinel subgroup (2-3 or 4-2) the sample belongs. The program also indicates the ratios of $\text{Fe}^{3+}/\text{Fe}^{2+}$, $\text{Fe}^{3+}/(\text{Fe}^{2+} + \text{Fe}^{3+})$, $\text{Cr}/(\text{Cr} + \text{Al})$, $\text{Fe}^{2+}/(\text{Fe}^{2+} + \text{Mg})$, $\text{Cr}/(\text{Cr} + \text{Al} + \text{Fe}^{3+})$ and $\text{Ti}/(\text{Ti} + \text{Cr} + \text{Al})$, among others, which can be used for the 2D projections of the magnetite prism (composed of six end-members of the group (2-3), magnetite, spinel, chromite, magnesiochromite, hercynite, magnesioferrite). However, in some cases it is not correct to use these ratios, for example, for coulsonite (FeV_2O_4 , S1 Table 3 from Yavuz and Yavuz, 2023), with ratios of $\text{Cr}/\text{Cr} + \text{Al} = 0.94$ and $\text{Cr}/(\text{Cr} + \text{Al} + \text{Fe}^{3+}) = 0.92$. These ratios could be plotted in the corresponding 2D triangular and binary graphs, although it is a mineral species that should not be included there because the dominant B cation is V. OxyEMG, as explained before, considers ΣR^{2+} ($\text{Fe}^{2+} + \text{Mg}$) and ΣR^{3+} ($\text{Cr} + \text{Al} + \text{Fe}^{3+}$) to know which samples can be plotted in the magnetite or ulvöspinel prisms.

6 Conclusions

OxyEMG is an improved version of the EMG application that allows for calculating the 31 end-members of the oxyspinel group, based on data obtained with EMPA. An important addition, among others, is that it also allows for obtaining redistribution proportions for the corresponding end-members in the magnetite or ulvöspinel prisms and a data validation section to check the results.

Code availability. The application was implemented in the Unity engine (Unity Technologies, 2005) and can be freely downloaded at the following link: <http://vyglab.cs.uns.edu.ar/webpage/index.php/es/recurcos/oxiyemg> (Ferracutti et al., 2024).

The users are kindly requested to give appropriate credit to this article in their publications if Oxyspinel group End-Member Generator (OxyEMG) has been used to perform calculations.

Data availability. All raw data can be provided by the corresponding authors upon request.

Supplement. The supplement related to this article is available online at: <https://doi.org/10.5194/ejm-36-87-2024-supplement>.

Author contributions. GRF made all the calculations necessary to obtain cation proportions (p.f.u., per formula unit), 31 end-

members of the oxyspinel group, the ΣR^{3+} value, the ΣR^{2+} value, $\Sigma R^{3+} / \Sigma R^{2+}$ ratios, redistribution proportions for the corresponding end-members in the magnetite or ulvöspinel prisms, and data validation. GRF: conceptualization, methodology, writing (original draft and review and editing). LMA: conceptualization, methodology, writing (original draft and review and editing). ASA and MLG: application creation, writing original draft. JET: conceptualization, methodology. All authors reviewed the manuscript.

Competing interests. The contact author has declared that none of the authors has any competing interests.

Disclaimer. Publisher's note: Copernicus Publications remains neutral with regard to jurisdictional claims made in the text, published maps, institutional affiliations, or any other geographical representation in this paper. While Copernicus Publications makes every effort to include appropriate place names, the final responsibility lies with the authors.

Special issue statement. This article is part of the special issue "New minerals: EJM support". It is not associated with a conference.

Acknowledgements. The authors are grateful to Silvia Castro and Ernesto Bjerg for their helpful and constructive comments and suggestions. The authors thank Andrew Christy; two anonymous reviewers; and the editors, Cristian Biagioni (associate editor) and Sergey Krivovichev (chief editor), for their constructive comments and suggestions which significantly improved this work.

Financial support. This work was financed by project 24/H148 granted to Gabriela R. Ferracutti by the General Secretariat of Science and Technology of the Universidad Nacional del Sur.

Review statement. This paper was edited by Cristian Biagioni and reviewed by Andrew Christy and two anonymous referees.

References

Antao, S. M., Cruickshank, L. A., and Hazrah, K. S.: Structural Trends and Solid-Solutions Based on the Crystal Chemistry of Two Hausmannite (Mn_3O_4) Samples from the Kalahari Manganese Field, *Minerals*, 9, 343, <https://doi.org/10.3390/min9060343>, 2019.

Anthony, J. W., Bideaux, R. A., Bladh, K. W., and Nichols, M. C.: *Handbook of Mineralogy*, Mineralogical Society of America, Chantilly, USA, <http://www.handbookofmineralogy.org/> (last access: 11 September 2023), 2001–2005.

Bjerg, E. A., de Brodtkorb, M., and Stumpfl, E. F.: Compositional zoning in Zn-chromites from the Cordillera

Frontal Range, Argentina, *Mineral. Mag.*, 57, 131–139, <https://doi.org/10.1180/minmag.1993.057.386.13>, 1993.

Bosi, F., Lucchesi, S., and Della Giusta, A.: Structural relationships in $(Mn_{1-x}Zn_x)Mn_2O_4$ ($0 \leq x \leq 0.26$): The “dragging effect” of the tetrahedron on the octahedron, *Am. Mineral.*, 87, 1121–1127, <https://doi.org/10.2138/am-2002-8-909>, 2002.

Bosi, F., Hålenius, U., Andreozzi, G. B., Skogby, H., and Lucchesi, S.: Structural refinement and crystal chemistry of Mn-doped spinel: A case for tetrahedrally coordinated Mn^{3+} in an oxygen-based structure, *Am. Mineral.*, 92, 27–33, <https://doi.org/10.2138/am.2007.2266>, 2007.

Bosi, F., Hålenius, U., and Skogby, H.: Crystal chemistry of the magnetite-ulvöspinel series, *Am. Mineral.*, 94, 181–189, <https://doi.org/10.2138/am.2009.3002>, 2009.

Bosi, F., Hålenius, U., and Skogby, H.: Crystal chemistry of the $MgAl_2O_4$ - $MgMn_2O_4$ - $MnMn_2O_4$ system: Analysis of structural distortion in spinel- and hausmannite-type structures, *Am. Mineral.*, 95, 602–607, <https://doi.org/10.2138/am-2016-5508>, 2010.

Bosi, F., Hålenius, U., and Skogby, H.: Crystal chemistry of the ulvöspinel-qandilite series, *Am. Mineral.*, 99, 847–851, <https://doi.org/10.2138/am.2014.4722>, 2014.

Bosi, F., Biagioni, C., and Pasero, M.: Nomenclature and classification of the spinel supergroup, *Eur. J. Mineral.*, 31, 183–192, <https://doi.org/10.1127/ejm/2019/0031-2788>, 2019.

De Waal, S. A.: Nickel minerals from Barberton, South Africa: VIII. The spinels cochromite and nichromite, and their significance to the origin of the Bon Accord nickel deposit, *Bull. Bur. Rech. Geol. Minieres Sec. II Geol. Gites Mineraux*, 3, 225–230, 1978.

Dolivo-Dobrovolsky, V. V.: Dominant Valency, End Members, and Reciprocal Systems, *Geol. Ore Depos.*, 52, 618–623, <https://doi.org/10.1134/S1075701510070123>, 2010.

Droop, G. T. R.: A General equation for estimating Fe^{3+} concentrations in ferromagnesian silicates and oxides from microprobe analyses, using stoichiometric criteria, *Mineral. Mag.*, 51, 431–435, <https://doi.org/10.1180/minmag.1987.051.361.10>, 1987.

Ferracutti, G. R., Gargiulo, M. F., Ganuza, M. L., Bjerg, E. A., and Castro, S. M.: Determination of the spinel group end-members based on electron microprobe analyses, *Mineral. Petrol.*, 109, 153–160, <https://doi.org/10.1007/s00710-014-0363-1>, 2015.

Ferracutti, G. R., Asiain, L. M., Antonini, A. S., Tanzola, J. E., and Ganuza, M. L.: Oxy-EMG (End Members Generator of the OXYSpinel Group), *vyglab* [code], <http://vyglab.cs.uns.edu.ar/webpage/index.php/es/recursos/oxyemg>, last access: 12 January 2024.

Gutzmer, J., Beukes, N. J., Kleyenstüber, A. S. E., and Burger, A. M.: Magnetic hausmannite from hydrothermally altered manganese ore in the paleoproterozoic kalahari manganese deposit, Transvaal Supergroup, South Africa, *Mineral. Mag.*, 59, 703–716, <https://doi.org/10.1180/minmag.1995.059.397.12> 1995.

Hatert, F. and Burke, E. A. J.: The IMA–CNMNC dominant constituent rule revisited and extended, *Can. Mineral.*, 46, 717–728, <https://doi.org/10.3749/canmin.46.3.717>, 2008.

Hwang, S. L., Shen, P., Yui, T. F., Chu, H. T., Iizuka, Y., Schertl, H. P., and Spengler, D.: Chihmingite, IMA 2022-010, in: CNMNC Newsletter 67, *Eur. J. Mineral.*, 34, <https://doi.org/10.5194/ejm-34-359-2022>, 2022.

Kompanchenko, A. A.: Coulsonite FeV_2O_4 – A rare vanadium spinel group mineral in metamorphosed massive sul-

- fide ores of the Kola Region, Russia, *Minerals*, 10, 843, <https://doi.org/10.3390/min10100843>, 2020.
- Lei, Z., Chen, X., Wang, J., Huang, Y., Du, F., and Yan Z.: Guite, the spinel-structured $\text{Co}^{2+}\text{Co}_2^{3+}\text{O}_4$, a new mineral from the Sicomines copper-cobalt mine, Democratic Republic of Congo, *Mineral. Mag.*, 86, 346–353, <https://doi.org/10.1180/mgm.2022.27>, 2022.
- Lenaz, D., O'Driscoll, B., and Princivale, F.: Petrogenesis of the anorthosite-chromitite association: crystal-chemical and petrological insights from the Rum Layered Suite, NW Scotland, *Contrib. Mineral. Petr.*, 162, 1201–1213, <https://doi.org/10.1007/s00410-011-0647-y>, 2011.
- Nepal, R. K.: Investigation of Complex Magnetic Phenomena in Spinel FeMn_2O_4 , MnFe_2O_4 , and NiFe_2O_4 , LSU Doctoral Dissertations, 5190, https://repository.lsu.edu/gradschool_dissertations/5190 (last access: September 2023), 2020.
- Oktyabrsky, R. A., Shcheka, S. A., Lennikov, A. M., and Afanasyeva, T. B.: The first occurrence of qandilite in Russia, *Mineral. Mag.*, 56, 385–389, <https://doi.org/10.1180/minmag.1992.056.384.11>, 1992.
- Unity Technologies: Unity Engine, <https://unity.com> (last access: October 2023), 2005.
- Yavuz, F. and Yavuz, V.: WinSpingc, a Windows program for spinel supergroup minerals, *J. Geosci.*, 68, 95–110, <https://doi.org/10.3190/jgeosci.369>, 2023.